THE UNIVERSITY OF WARWICK

Original citation:
Dobrzanska, Dorota A, Cooper, Amy L., Dowson, Christopher G., Evans, Stephen D., Haynes, Tommy, Johnson, Benjamin R. G., Stec, Helena M., Taylor, Paul C. and Marsh, Andrew Protein-adhesive and protein-resistant functionalized silicon surfaces. Langmuir .ISSN 0743-7463 (Submitted)
Permanent WRAP url:
http://wrap.warwick.ac.uk/62786

A note on versions:
The version presented here is a working paper or pre-print that may be later published elsewhere. If a published version is known of, the above WRAP url will contain details on finding it.

For more information, please contact the WRAP Team at: publicatons@warwick.ac.uk

Protein-adhesive and protein-resistant functionalized silicon surfaces.

Dorota A. Dobrzanska,[b,c] *Amy L. Cooper,*[‡b] *Christopher G. Dowson,*[c] *Stephen D. Evans,*[a] *Tommy Haynes,*[‡b] *Benjamin R. Johnson,*[a] *Helena M. Stec,*[b] *Paul C. Taylor,*[b] *Andrew Marsh.**[b]

[a] School of Physics and Astronomy, University of Leeds, Leeds, LS2 9JT, United Kingdom; Tel: +44 113 343 3807; E-mail: s.d.evans@leeds.ac.uk

[b] Department of Chemistry, University of Warwick, Coventry, CV4 7AL, United Kingdom, Fax: +44 24 7652 4112; Tel: +44 24 7652 4565; E-mail: a.marsh@warwick.ac.uk

[c] School of Life Sciences, University of Warwick, Coventry, CV4 7AL, United Kingdom, Tel: +44 24 7652 3534; E-mail: c.g.dowson@warwick.ac.uk

KEYWORDS: etched silicon, XPS, AFM, lysozyme, fibrinogen, protein adhesion, protein resistance

ABSTRACT

A series of new ω-alkenyl tertiary amine *N*-oxides is prepared in solution and immobilized on hydrofluoric acid-etched silicon {111} wafers. These monolayers are characterized by X-ray photoelectron spectroscopy, contact angle measurements, atomic force microscopy (AFM) and tested for their resistance to non-specific protein adhesion with two model proteins, lysozyme and fibrinogen. The use of silicon substrates is found to give good quality tertiary amine *N*-oxide

monolayers and these new surfaces are found to be significantly better at preventing non-specific protein adhesion than their parent amines as judged by AFM imaging.

1. INTRODUCTION

Engineered semiconductor, porous silicon and related surfaces provide an important means of linking microelectronics with the world we experience around us and hence are pivotal in current and future sensor technologies.[1-3] Selective deposition on Si / SiO_2 of peptides,[4, 5] nucleic acids,[6] modified nucleobases[7] and nanotubes[8] play an important role in manipulating the energy levels (work function) of the underlying semiconductor [9, 10] and selectively controlling the adhesion of subsequent layers, including cells.[11]

We have previously shown that tertiary amine *N*-oxides are more effective than their parent amines in resisting adhesion of proteins and phage,[12, 13] and provide a biocompatible environment at an interface. These amphiphiles are believed to show reasonably low toxicity, finding application in household products,[14] are known to be useful for DNA transfection,[15, 16] and in manipulating and crystallizing membrane proteins.[17] They are typically prepared by oxidation of a tertiary amine using hydrogen peroxide or meta-chloroperbenzoic acid (m-CPBA).[18] In solution chemistry we remove excess oxidant by addition of an electron-rich alkene.[19] We demonstrate herein that straightforward photoinitiated chemistry[20-22] is an ideal method for creating self-assembled monolayers of a small library of tertiary amine *N*-oxides on etched, hydrogen terminated silicon,[23] and that they provide a significantly different environment for proteins compared to corresponding tertiary amines.

2. EXPERIMENTAL SECTION

2.1. Materials. Reagents were purchased from Aldrich and used as supplied unless otherwise stated. All solvents were purchased from Fisher and were used as supplied unless otherwise stated. N-type silicon {111} wafers were obtained from the NanoSilicon Group, Department of Physics, University of Warwick. Brockmann grade II/III alumina was prepared by adding 5% water by weight dropwise to neutral Brockmann grade I alumina with constant swirling. UV initiated silicon wafer derivations was carried out using 254 nm light from a UVP MRL 58 Multiple-Ray Lamp. Water used for measurements including contact angle and critical micelle concentration refers to MilliQ® water. Lysozyme from chicken white egg and fibrinogen from human plasma were purchased from Sigma-Aldrich (Molecular Biology grade). Amines and amine *N*-oxides were prepared following the procedures 2.2-2.3.

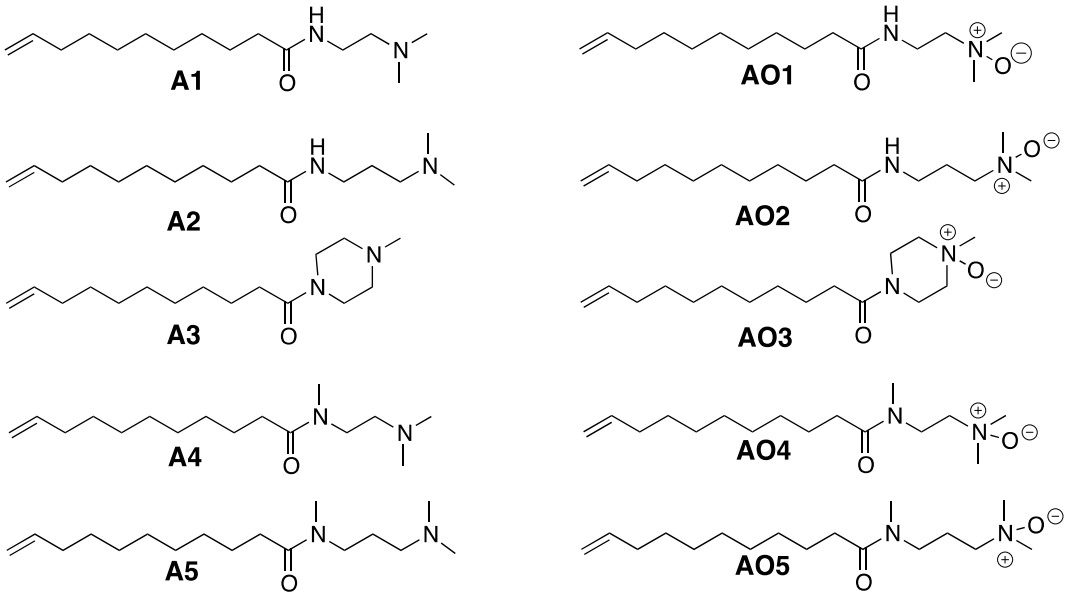

Figure 1. Amines **A1-A5** and amine oxides **AO1-AO5** prepared to functionalize N-type silicon {111} wafers.

2.2. General procedure A. Schotten – Baumann conditions to prepare *tertiary amines*, **A1-A5**.

To a rapidly stirred biphasic solution of undecenoyl chloride (1 eq.) in CH_2Cl_2 (40 ml) and 1M NaOH (aq) at 0 °C was added *primary amine* (1 eq.) in CH_2Cl_2 (9 mL). The reaction was stirred at 0 °C for 1 h then allowed to warm to room temperature, whereupon the two phases were separated and the organic layer was washed with water (x3) and dried over $MgSO_4$. The solvent was removed under reduced pressure and the resulting oil purified by silica flash chromatography (10:1 CH_2Cl_2:MeOH) to give the *products* **A1** – **A5**.

Analytical Data:

General procedure **A** was used with *N*,*N*-dimethyl-1,2-ethanediamine (1.61 g, 18.3 mmol, 1 eq.) to yield *N*-[2'-(dimethylamino)ethyl]undec-10-enamide **A1** as yellow oil (2.55 g, 54 %) R_f = 0.42, silica (10:1:0.5 CH_2Cl_2:MeOH:NH_3); ν_{max} (film) 3295 (N-H stretch), 2925 (C-H str.), 2854 (C-H str.), 1641 (C=O str.), 1547 (C-N str.), 1459 (C-H def.) cm^{-1}; ^1H NMR ($CDCl_3$, 400 MHz): 1.19-1.38 (m, 10H, H^4, H^5, H^6, H^7, H^8), 1.62 (m, 2H, H^3), 2.03 (m, 2H, H^9), 2.09 (t, 2H, J = 7.5 Hz, H^2), 2.23 (s, 6H, 2 x $H^{4'}$), 2.40 (m, 2H, $H^{3'}$), 3.32 (q, 2H, J = 5.5 Hz, $H^{2'}$), 4.82-4.97 (m, 2H, H^{10}), 3.64-5.86 (ddt, 1H, J = 17 Hz, 10 Hz, 6.5 Hz, H^{11}), 6.09 (s, 1H, NH) ppm; ^{13}C NMR ($CDCl_3$, 75 MHz): 25.7 (C^3), 28.8-29.2 (C^4, C^5, C^6, C^7, C^8), 33.7 (C^9), 36.6 (C^2), 41.4 ($C^{2'}$), 45.6 (2x$C^{4'}$), 57.8 ($C^{3'}$), 114.1 (C^{11}), 139.2 (C^{10}), 173.2 (C^1) ppm; LSMS *m/z*: $[M+H]^+$ 255. 2 (100%); HRMS *m/z*: calculated $[M+H]^+$ $C_{15}H_{30}ON_2$ = 255.2436, found = 255.2427 $[M+H]^+$.

General procedure **A** was used with *N*,*N*-dimethyl-1,3-propyldiamine (1.62 g, 15.9 mmol) to yield *N*-[3'-(dimethylamino)propyl]undec-10-enamide **A2** as a yellow oil (2.41 g, 56%) R_f = 0.37, silica (10:1:0.5 CH_2Cl_2: MeOH:NH_3); ν_{max} (film) = 3289 (N-H str.), 2925 (C-H str.), 2854 (C-H str.), 1641 (C=O str.), 1547 (C-N str.), 1460 (C-H def.) cm^{-1}; ^1H NMR ($CDCl_3$, 400 MHz) 1.22-1.41 (m, 10H, H^4, H^5, H^6, H^7, H^8); 1.51-1.65 (m, 2H, H^3); 2.02 (m, 2H, H^9); 2.14 (m, 2H,

$H^{3'}$); 2.22 (s, 6H, 2 x $H^{4'}$); 2.37 (t, 2H, J = 7 Hz, $H^{2'}$), 3.23-3.32 (q, 2H, J = 6 Hz, $H^{1'}$), 4.84-4.97 (m, 2H, H^{11}); 5.71-5.93 (ddt, 1H, J = 17,Hz, 10,Hz, 6.5 Hz, H^{10}) 7.03 (s, 1H, NH) ppm; ^{13}C NMR ($CDCl_3$, 75 Hz) 25.1 (C^3), 26.5 ($C^{2'}$), 28.2-28.6 (C^4, C^5, C^6, C^7, C^8), 33.1 (C^9), 36.3 ($C^{1'}$), 38.5 (C^2), 45.4 (2x$C^{4'}$), 57.9 ($C^{2'}$), 113.5 (C^{11}), 138.7 (C^{10}), 172.5 (C^1) ppm; LRMS *m/z*: $[M+H]^+$ 269.4 (100%) HRMS *m/z* calculated $[M+H]^+$ $C_{16}H_{32}ON_2$ = 269.2587, found = 269.2569 $[M+H]^+$.

General procedure **A** was used with 1-methylpiperazine (1.81 g, 18.0 mmol) to yield 1-(4'-methylpiperazin-1'-yl)undec-10-en-1'-one **A3** as an orange oil (3.31 g, 69 %); R_f = 0.32, silica (10:1:0.5 CH_2Cl_2: MeOH:NH_3); ν_{max} (film) = 3076 (C=C-H str.), 2924 (C-H str.), 2853 (C-H str.), 2791 (C-N str.) 1640 (C=O str.), 1528 (C-N str.), 1431 (C-H def.) cm^{-1}; ^1H NMR ($CDCl_3$, 400 MHz) 1.22-1.41 (m, 10H, H^4, H^5, H^6, H^7, H^8); 1.49-1.60 (m, 2H, H^3); 2.02 (m, 2H, H^9); 2.16-2.39 (m, 10H, H^2, $H^{3'ax}$, $H^{3'eq}$, H^3); 2.30 (s, 3H, NMe ($H^{5'}$)), 3.47 (dd, 2H, J = 8 Hz, 6.5 Hz, $H^{2',2''eq}$); 3.61 (dd, 2H, J = 8.5 Hz, 6.5 Hz, $H^{2',2''ax}$); 4.84-4.97 (m, 2H, H^{11}); 5.84 (ddt, 1H, J = 17 Hz, 10 Hz, 6.5 Hz, H^{10}) ppm; ^{13}C NMR ($CDCl_3$, 75 MHz) 24.7 (C^3), 28.2-28.8 (C^4, C^5, C^6, C^7, C^8), 32.7 (C^9), 33.2 (C^2), 41.8 ($C^{2'}$), 44.8 ($C^{2''}$), 45.2 (NMe $C^{5'}$), 54.1 ($C^{3'}$ and $C^{3''}$), 113.5 (C^{11}), 138.4 (C^{10}), 174.2 (C^1) ppm; LRMS *m/z*: $[M+H]^+$ 267.2 (100%); HRMS *m/z* calculated $[M+H]^+$ $C_{16}H_{30}ON_2$ = 267.2436, found = 267.2425 $[M+H]^+$.

General procedure **A** was used with *N,N,N'*-trimethyl-1,2-ethanediamine (1.6 g, 15.7 mmol) to yield *N*-[2'-(dimethylamino)ethyl]-*N*-methylundec-10-enamide **A4** as a yellow oil (2.13 g, 51 %); R_f = 0.35, silica (10:1:0.5 CH_2Cl_2:MeOH:NH_3); ν_{max} (film) 3075 (C=CH str.), 2925 (C-H str.), 2854 (C-H str.), 1641 (C=O str.), 1528 (C-N str.), 1431 (C-H def.) cm^{-1}; ^1H NMR ($CDCl_3$,

400 MHz): 1.18-1.38 (m, 10H, H^4, H^5, H^6, H^7, H^8), 1.62 (m, 2H, H^3), 2.03 (m, 2H, H^9), 2.12-2.27 (m, 2H, $H^{1'}$, $H^{2'}$), 2.26 (s, 6H, $H^{3'}$), 2.94 (s, rotamers 3H, $H^{4'}$), 3.01 (s, rotamers 3H, $H^{4''}$), 3.24-3.38 (t, 2H, J = 7 Hz, $H^{1'}$), 3.45-3.61 (t, 2H, J = 7 Hz, $H^{2'}$), 4.82-4.98 (m, 2H, H^{11}), 5.64-5.86 (ddt, 1H, J = 17 Hz, 10 Hz, 6.5 Hz, H^{10}) ppm; ^{13}C NMR ($CDCl_3$, 75 MHz): 24.4 (C^3), 28.8-29.2 (C^4, C^5, C^6, C^7, C^8), 33.2 (C^9), 35.3 ($C^{4'}$), 45.0 ($C^{3'}$), 45.1 (C^2), 47.8 ($C^{1'}$), 56.1 ($C^{2'}$), 114.1 (C^1), 138.6 (C^{10}), 172.5 (C^1) ppm; LRMS *m/z*: $[M+H]^+$ 269.4 (100%); HRMS *m/z* calculated $[M+H]^+$ $C_{16}H_{32}ON_2$ = 269.2577, found = 269.2587 $[M+H]^+$.

General procedure **A** was used with *N,N,N'*-trimethyl-1,3-propanediamine (1.58 g, 13.6 mmol) to yield *N*-[3'-(dimethylamino)propyl]-*N*-methylundec-10-enamide **A5** as a yellow oil (2.46 g, 64 %) R_f = 0.35, silica (10:1:0.5 CH_2Cl_2:MeOH:NH_3); v_{max} (film) 3075 (C=CH str.), 2925 (C-H str.), 2854 (C-H str.), 1641 (C=O str.), 1528 (C-N str.), 1431 (C-H def.) cm^{-1}; ^1H NMR ($CDCl_3$, 400 MHz): 1.15-1.35 (m, 10H, H^4, H^5, H^6, H^7, H^8), 1.47-1.73 (m, 4H, $H^{2'}$, $H^{3'}$), 1.88-1.9 (m, 2H, H^9), 2.10-2.29 (m, 10H, H^2, $H^{3'}$, $H^{4'}$), 2.8 (s, rotamer, 3H, $H^{5'}$), 2.9 (s, rotamer, 3H, $H^{5''}$), 3.19 (m, rotamer, 2H, $H^{1'}$), 3.45 (m rotamer, 2H, $H^{1'}$), 4.79-4.95 (m, 2H, H^{11}), 5.64-5.86 (ddt, 1H, J = 17 Hz, 10 Hz, 6.5 Hz, H^{10}) ppm; ^{13}C NMR ($CDCl_3$, 75 MHz): 24.8 (C^3), 26.0 ($C^{2'}$), 28.2-28.8 (C^4, C^5, C^6, C^7, C^8), 33.1 (C^9), 34.9 ($C^{4'}$), 44.7 ($C^{3'}$), 45.3 (C^2), 47.1 ($C^{1'}$), 56.3 ($C^{2'}$), 113.8 (C^{11}), 138.6 (C^{10}), 172.5 (C^1) ppm; LRMS *m/z*: $[M+H]^+$ 283.3 (100%) HRMS *m/z* calculated $[M+H]^+$ $C_{17}H_{34}ON_2$ = 283.2765, found = 283.2767 $[M+H]^+$.

2.3. General procedure B. Oxidation of amines to yield compounds **AO1-AO5.**

To a dry three-necked round bottom flask under nitrogen atmosphere was added potassium carbonate (1.54 g, 11.00 mmol, 2.3 eq), and a solution of *tertiary amine* (1 eq.) in CH_2Cl_2 (20

ml) with stirring, and cooled to –78 ºC. A solution of 50-89% m-CPBA (1.30 g, 7.60 mmol, 1.6 eq.) in CH_2Cl_2 (20 ml) was added *via* syringe and the reaction stirred vigorously for 3 hours after which time any remaining m-CPBA was removed by addition of limonene (*d* = 0.84, 0.62 ml, 3.80 mmol, 0.8 eq.) *via* syringe over 10 mins. The reaction mixture was filtered through Florisil®, washed with 4:1 CH_2Cl_2:MeOH and solvent removed by reduced pressure. The residue was purified over a column of neutral alumina Brockmann grade II/III eluted with 5:1 CH_2Cl_2:MeOH, to give, after removal of solvent under reduced pressure, *products* **AO1** – **AO5**.

Analytical Data:

General procedure **B** was used with *N*-[2'-(dimethylamino)ethyl]undec-10-enamide **A1** (1.18 g, 4.65 mmol) to yield *N*-[2'-(dimethylamine *N*-oxide)ethyl]undec-10-enamide **AO1** as a white solid (0.80 g, 64%), m.p. 95-97 °C; R_f = 0.41, neutral alumina (10:1:0.5 CH_2Cl_2: MeOH: NH_3); v_{max} (film): 3284 (N-H), 3077 (C=CH str.), 2924 (C-H str.), 2854 (C-H str.), 1642 (C=O str.), 1545 (C-H def.), 961 (N^+-O^- str.) cm^{-1}; ^1H NMR ($CDCl_3$, 400 MHz): 1.24-1.48 (m, 10H, H^4, H^5, H^6, H^7, H^8), 1.56-1.71 (m, 2H, H^3), 2.06 (m, 2H, H^9), 2.21 (m, 2H, H^2), 3.28 (s, 6H, 2x$H^{3'}$), 3.51 (m, 2H, $H^{2'}$), 3.72 (m, 2H, $H^{1'}$), 4.89 (m, 2H, H^{11}), 5.72-5.91 (ddt, 1H, *J* = 17 Hz, 10 Hz, 6.5 Hz, H^{10}), 7.95 (s, 1H, NH) ppm; ^{13}C NMR ($CDCl_3$, 75 MHz): 26.8 (C^3), 30.1-30.4 (C^4, C^5, C^6, C^7, C^8), 34.9 (C^9), 35.1 (C^1), 37.0 (C^2), 58.8 ($C^{2'}$), 69.4 ($C^{1'}$), 114.8 (C^{11}), 139.5 (C^{10}), 176.6 (C^1) ppm; LSMS *m/z*: $[M+H]^+$ 271.7(100%); HRMS *m/z* calculated $[M+H]^+$ $C_{15}H_{30}O_2N_2$ = 271.2361, found = 271.2381 $[M+H]^+$.

General procedure **B** was used with *N*-[3'-(dimethylamino)propyl]undec-10-enamide **A2** (2.2 g, 8.21 mmol) to yield *N*-[3'-(dimethylamine *N*-oxide)propyl]undec-10-enamide **AO2** as a

white/yellow solid (1.4 g, 61%), m.p. 97-99 °C; R_f = 0.43, neutral alumina (10:1:0.5 CH_2Cl_2: MeOH: NH_3); ν_{max} (film): 3278 (N-H), 3077 (C=CH str.), 2925 (C-H str.), 2854 (C-H str.), 1643 (C=O str.), 1543 (C-H def.), 903 (N^+-O^- str.) cm^{-1}; ^1H NMR ($CDCl_3$, 400 MHz): 1.27-1.45 (m, 10H, H^4, H^5, H^6, H^7, H^8), 1.62 (m, 2H, H^3), 2.03 (m, 2H, H^9), 2.22 (m, 2H, H^2), 3.17 (s, 6H, 2x$H^{4'}$), 3.34 (m, 4H, $H^{1'}$, $H^{3'}$), 4.88 -5.02 (m, 2H, H^{11}), 5.72-5.91 (ddt, 1H, *J* = 17 Hz, 10 Hz, 6.5 Hz, H^{10}), 7.95 (s, 1H, NH) ppm; ^{13}C NMR ($CDCl_3$, 75 MHz): 24.8 (C^3), 26.9 ($C^{2'}$), 30.1-30.4 (C^4, C^5, C^6, C^7, C^8), 34.9 (C^9), 37.1 ($C^{1'}$), 37.5 (C^2), 58.7 ($C^{4'}$), 69.4 ($C^{3'}$), 114.7 (C^{11}), 139.2 (C^{10}), 173.3 (C^1) ppm; LSMS *m/z*: $[M+H]^+$ 285.4 (100%); HRMS *m/z* calculated $[M+H]^+$ $C_{16}H_{32}O_2N_2$ = 285.2542, found = 285.2537 $[M+H]^+$.

General procedure **B** was used with 1-(4'-methylpiperazin-1'-yl-4'-amine)undec-10-en-1'-one **A3** (2.45 g, 9.21 mmol) to yield 1-(4'-methylpiperazin-1'-yl-4'-amine *N*-oxide)undec-10-en-1'-one **AO3** as a white solid (1.98 g, 76%), m.p. 95-97 °C; R_f = 0.41, neutral alumina (10:1:0.5 CH_2Cl_2: MeOH: NH_3), ν_{max} (film) 3079 (C=C-H str.), 2922 (C-H str.), 2852 (C-H str.), 2793 (C-N str.) 1639 (C=O str.), 1530 (C-N str.), 1434 (C-H def.), 974 (N^+-O^- str.) cm^{-1}; ^1H NMR ($CDCl_3$, 400 MHz) 1.29-1.46 (m, 10H, H^4, H^5, H^6, H^7, H^8); 1.56-1.67 (m, 2H, H^3); 1.98 (m, 2H, H^9); 2.26 (m, 2H, H^2); 3.18-3.24 (m, 4H, $H^{2'eq}$, $H^{3'eq}$ and $H^{2''eq}$, $H^{3''eq}$); 3.21 (s, 3H, N-Me ($H^{5'}$)); 3.38-4.49 (m, 2H, $H^{3''ax}$ and $H^{3'ax}$), 4.04 (m, 1H, $H^{2''ax}$), 4.51 (m, 1H, $H^{2'ax}$) 4.99 (m, 2H, H^{11}); 5.72- 5.90 (ddt, 1H, *J* = 17 Hz, 10 Hz, 6.5 Hz, H^{10}) ppm; ^{13}C NMR ($CDCl_3$, 75 Hz) 26.3 (C^3), 30.1-30.5 (C^4, C^5, C^6, C^7, C^8), 33.8 (C^9), 34.9 (C^2), 41.9, 37.4 ($C^{1'}$ and $C^{1''}$) , 60.7 ($C^{3'}$), 66.1, 65.9 ($C^{2'}$ and $C^{2''}$), 113.5 (C^{11}), 139.2 (C^{10}) 174.2 (C^1) ppm; LRMS *m/z:* $[M+H]^+$ 283.2; HRMS *m/z* calculated $[M+H]^+$ $C_{16}H_{30}O_2N_2$ = 283.2386, found = 283.2371 $[M+H]^+$.

General procedure **B** was used with *N*-[2'-(dimethylamine)ethyl]-*N*-methylundec-10-enamide **A4** (2.35 g, 8.77 mmol) to yield *N*-[2'-(dimethylamine *N*-oxide)ethyl]-*N*-methylundec-10-enamide **AO4** as a white solid (1.43 g, 57%), m.p. 96-98 °C; R_f = 0.35, neutral alumina (10:1:0.5 CH_2Cl_2: MeOH: NH_3); v_{max} (film) 3075 (C=CH str.), 2925 (C-H str.), 2850 (C-H str.), 1637 (C=O str.), 1534 (C-N str.), 1458 (C-H def.) 974 (N^+-O^- str.) cm^{-1}; ^1H NMR ($CDCl_3$, 400 MHz): 1.29-1.46 (m, 10H, H^4, H^5, H^6, H^7, H^8), 1.62 (m, 2H, H^9), 2.06 (m, 2H, H^3), 2.38 (q, 2H, *J* = 7 Hz, H^2), 3.13 (s, rotamers, 3H, $H^{4'}$), 3.19 (s, rotamers, 3H, $H^{4''}$), 3.23 (s, 6H, $H^{3'}$), 3.45 (m, 2H, $H^{2'}$), 4.85-4.94 (2 x m, 2H, 2x$H^{1'}$), 4.96-5.05 (m, 2H, H^{11}), 5.64-5.82 (ddt, 1H, *J* = 17 Hz, 10 Hz, 6.5 Hz, H^{10}) ppm; ^{13}C NMR ($CDCl_3$, 75 MHz): 24.7 (C^3), 30.8-31.4 (C^4, C^5, C^6, C^7, C^8), 33.8 (C^9), 34.3 ($C^{4'}$), 36.4 (C^2) 42.9 ($C^{1'}$), 58.6 ($C^{3'}$), 67.6 ($C^{2'}$), 114.1 (C^{11}), 140.1 (C^{10}), 172.5 (C^1) ppm; LRMS *m/z*: $[M+H]^+$ 285.2 (100%); HRMS *m/z* calculated $[M+H]^+$ $C_{16}H_{32}O_2N_2$ = 285.2542, found = 285.2544 $[M+H]^+$.

General procedure **B** was used with *N*-[3'-(dimethylamine)propyl]-*N*-methylundec-10-enamide **A5** (2.4 g, 8.51 mmol) to yield *N*-[3'-(dimethylamine *N*-oxide)propyl]-*N*-methylundec-10-enamide **AO5** as a white solid (1.73 g, 68 %); m.p. 98-100 °C; R_f = 0.52, neutral alumina (10:1:0.5 CH_2Cl_2: MeOH: NH_3); v_{max} (film) 3077 (C=CH str.), 2924 (C-H str.), 2854 (C-H str.), 1642 (C=O str.), 1545 (C-N str.), 967 (N^+-O^- str.) cm^{-1}; ^1H NMR (MeOD, 400 MHz): 1.24-1.44 (m, 10H, H^4, H^5, H^6, H^7, H^8), 1.55-1.67 (m, 4H, $H^{2'}$, H^3), 2.05-2.20 (m, 5H, $H^{2'}$, H^9), 2.39 (m, 10H, H^2), 2.55 (s, rotamer, 3H, $H^{5'}$), 3.09 (s, (rotamer), 3H, $H^{5''}$), 3.29-3.34 (m, 2H, $H^{3'}$), 3.48 (m, 2H, $H^{1'}$), 3.8 (s, 6H, $H^{4'}$), 4.90-4.95 (m, 2H, H^{11}), 5.64-5.86 (ddt, 1H, *J* = 17 Hz, 10 Hz, 6.5 Hz, H^{10}) ppm; ^{13}C NMR (MeOD, 75 MHz): 22.6 ($C^{2'}$), 26.2 (C^3), 30.2-30.8 (C^4, C^5, C^6, C^7, C^8), 34.4 (C^2), 34.9 (C^{10}), 35.9 ($C^{5'}$), 45.3 ($C^{1'}$), 58.1 ($C^{4'}$), 113.8 (C^{11}), 140.6 (C^{10}), 171.3 (C^1) ppm;

LRMS *m/z*: $[M+H]^+$ 299.3 (100%); HRMS *m/z* calculated $[M+H]^+$ $C_{17}H_{34}O_2N_2$ = 299.2622, found = 299.2645 $[M+H]^+$.

2.4. Etching (hydrogen termination) of silicon wafers.

This procedure was carried out in a laboratory designed for work with hydrofluoric acid. Safety measures such as full-face masks, full-length aprons and heavy-duty nitrile gloves were used during this procedure. A 5% HF solution was made by diluting 50% HF (10 ml) into distilled water (90 ml) in a Teflon beaker. The silicon wafers were immersed in this solution for 5 min, then washed with distilled water, degassed ethanol (5 ml) and degassed toluene (5 ml) and dried with a gentle flow of nitrogen after each wash.

2.5. Functionalization of hydrogen terminated silicon surfaces.

The hydrogen terminated silicon wafers prepared above were placed in vials containing 2 mM solutions of the following amines (**A1**-**A5**) and amine oxides (**AO1**-**AO5**) in degassed toluene (10 ml). Each of these vials were irradiated at 254 nm for 20 minutes with a UV lamp then each silicon wafer removed from its solution, washed with toluene (5 ml) and dried under a gentle flow of nitrogen.

2.6. Water contact angle measurements.

Static and receding water contact angles were measured on a KRUSS Drop Shape Analyser 100 at room temperature. Each measurement was repeated 3 times and the Wilcoxon signed-rank test was used to estimate the validity of the contact angles. This is a nonparametric statistical hypothesis test for the case of two related measurements on a single sample.

2.7. Tensiometry

The pendant drop method was used to measure surface tension on a KRUSS Drop Shape Analyser 100 at room temperature. Each measurement was repeated 4 times and the data presented in Table 1 is an average of all measurements.

2.8. X-Ray photoelectron spectroscopy (XPS).

XPS measurements were performed using a VG Escalab 250 XPS with monochromated aluminium K-alpha X-ray source. The spot size was 500 μm with a power of 150W. Detailed spectra of individual peaks were taken at an energy of 20 eV. Binding energy was calibrated by setting the carbon 1s peak to 285eV. Detailed spectra had a Shirley background fitted to them and peaks were generated by using mixed Gaussian-Lorentzian data fitting with CASAXPS.

2.9. Protein deposition and Atomic Force Microscopy (AFM).

Solutions of phosphate buffered saline (PBS), fibrinogen (1 μM in PBS) and lysozyme (1 mM in PBS) were prepared fresh and sonicated for 20 minutes prior to the deposition experiments to remove any air from the solutions. The derivatised surfaces were immersed in protein solution at room temperature (20 - 25°C) and allowed to stand for 15 min. The surface was rinsed three times with PBS (10 mL) and then dried under a gentle stream of dry nitrogen gas. The silicon wafers were then imaged in air at room temperature in tapping mode using an Asylum Research MFP-3D atomic force microscope. Data were treated offline using MFP3D Igor Pro to produce the magnified images seen in Figures 5 – 9.

3. RESULTS AND DISCUSSION

3.1 Synthesis.

A representative set of ω-alkene substituted tertiary amines **A1 - A5** (**Figure 1**) were initially prepared by coupling undecenoic acid with primary or secondary amines using isobutyl chloroformate.[24] In the case of compounds **A3, A4, A5**, the presence of isobutyl chloroformate-derived impurities led to the preferred use of a classic acyl chloride intermediate.[25, 26]

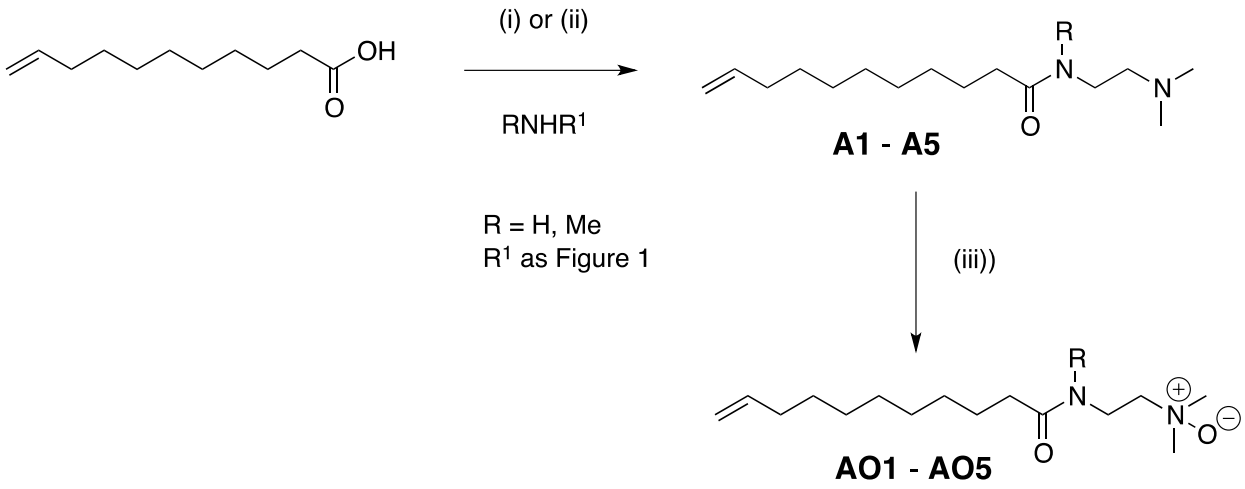

Scheme 1 *Reagents and conditions*: (i) isobutyl chloroformate, *N*-methylmorpholine, tetrahydrofuran, 0 °C; (ii) thionyl chloride, dimethylformamide, , CH_2Cl_2, r.t.; (iii) m-CPBA, K_2CO_3, CH_2Cl_2, -78 °C, then limonene -78 °C.

Removal of excess peroxide has been previously achieved[19] by bubbling 2-methylpropene for a few minutes at -78 °C, although the use of limonene as a sacrificial electron-rich alkene [27, 28] is here found to be a more easily conducted method with improved yield.

The product amine *N*-oxides displayed significant downfield ^{1}H NMR chemical shifts for those protons adjacent to this potent dipole. In the case of *N*-methyl piperazine adduct **AO3** the chemical shifts of individual pseudo-axial and pseudo-equatorial protons were especially

dramatic, moving from amine $H^{2'}$, $H^{2''}$ δ = 3.61 to exhibiting separate signals for the pseudo-axial protons $H^{2''}$ and $H^{2'}$ at δ = 4.04 and 4.51 ppm respectively, presumably due to desymmetrization of the 6-membered heterocycle by the two extreme conformations of the amide carbonyl that allow conjugation of the sp^2 amide nitrogen (**Figure 2**).

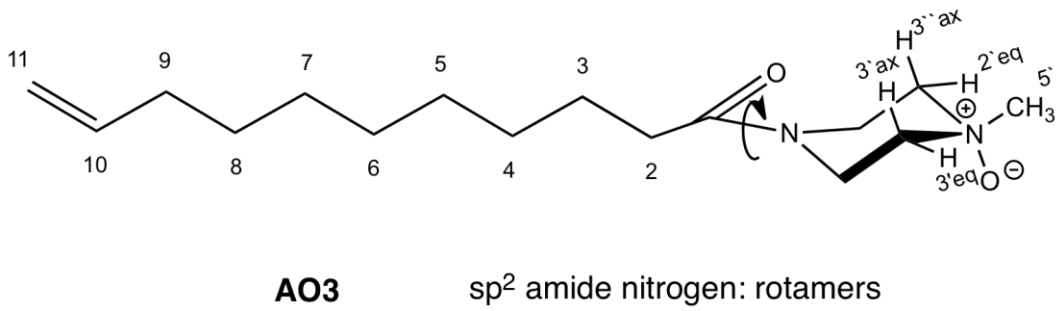

Figure 2: 1-(4'-methylpiperazin-1'-yl-4'-amine *N*-oxide)undec-10-en-1'-one **AO3**

3.2 Tensiometry measurements

The amphiphilic tertiary amines were analysed by tensiometry and a graph of surface tension versus log(concentration) (Supporting Information, Figure S2) enabled the critical aggregation concentration (CAC) for compounds **A1** – **A5** to be determined (**Table 1**).

Amines	**A1**	**A2**	**A3**	**A4**	**A5**
CAC (mM)	4.99	4.55	5.77	4.81	3.98

Table 1: Critical aggregation concentration for amines **A1** – **A5**.

By contrast, amine oxides **AO1** – **AO5** were all found to be too soluble to allow the determination of a CAC in the mM range.

3.3 Surface composition.

Once both series of amphiphiles, the tertiary amines and their cognate *N*-oxides had been immobilised on the freshly prepared silicon hydride-terminated wafers, X-ray photoelectron spectroscopy was used to confirm successful reaction. Functionalization of the surface in this way inhibits oxidation of the underlying silicon and enhances monolayer stability.[29] To confirm monolayer formation and surface composition, high-resolution carbon and nitrogen spectra were analyzed (**Figure 3**).

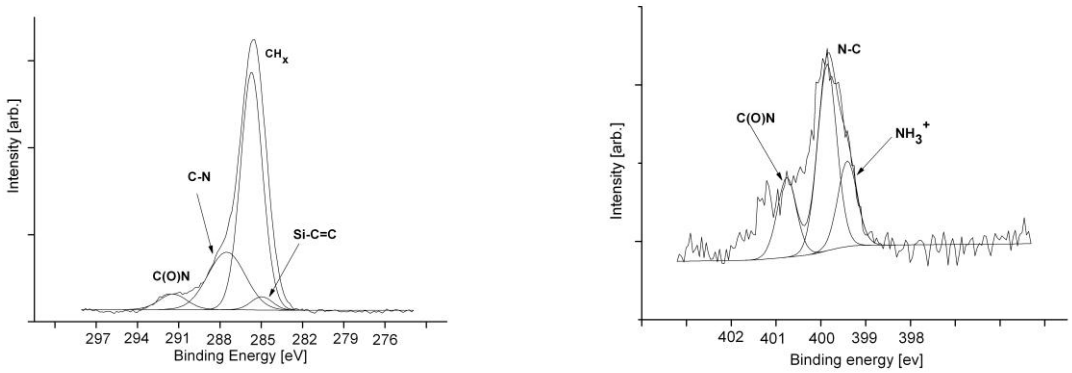

Figure 3 High-resolution carbon 1 s (left) and nitrogen 1s (right) XPS spectrographs for amine **A1**.

XPS narrow scan signals for carbon shows four peaks (a) predominant aliphatic chain carbon peak at 285 eV,[30] (b) a signal at 288 eV corresponding to N- and carbonyl bonded carbon,[31] (c) a signal at 291 eV assigned as amide C(O)N,[32] (d) a lower binding energy component at 285 eV assigned as Si-C=C.[33]

XPS narrow scan signals for nitrogen show in **Figure 3**: (a) a peak at 400.9 eV assigned to the amide moiety,[34] (b) a high energy signal at 400 eV for N-C,[35] (c) a signal at 399 eV assigned to the protonated amino group.[36]

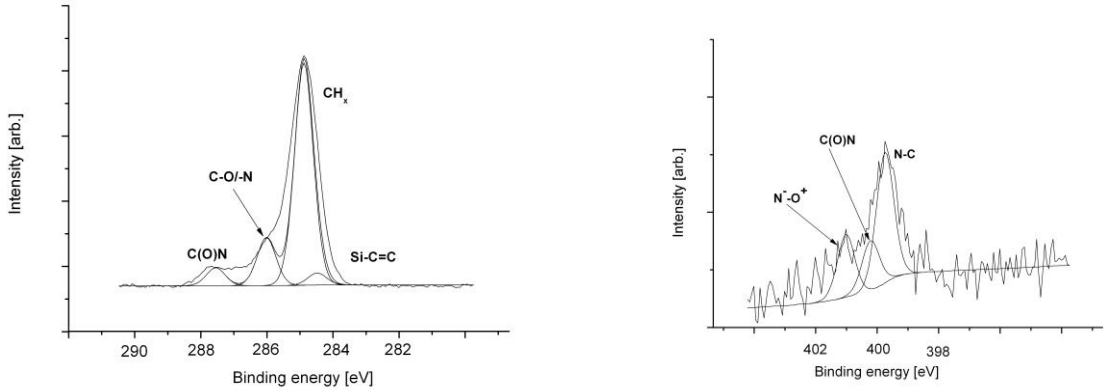

Figure 4 High-resolution carbon 1 s (left) and nitrogen 1s (right) XPS spectrographs for amine oxide **AO1**.

Carbon composition for the amine *N*-oxide is the same (**Figure 4**), however XPS scan for nitrogen shows (a) main peak at 400 eV assigned as N-C, (b) a peak at 400.5 eV assigned as amide and (c) a signal at 401 eV assigned as tertiary amine *N*-oxide.

3.4 Properties of the surfaces assessed by contact angle.

All the surfaces were examined by water droplet contact angle measurements performed in triplicate. The etched silicon surface is significantly more hydrophobic, indicating removal of hydroxyl functionality and the influence of the tertiary amine is clearly seen. The more hydrophilic amine *N*-oxide function is verified by the difference (Δ °) in subsequent contact angle.

Surface	Target structure	Average contact angle °	Δ °
Si	SiO_2	45.4 ± 0.7	-
Si + HF	Si-H	65.8 ± 0.8	-
A1	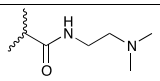	36.5 ± 0.8	-
AO1	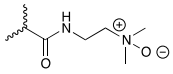	26.9 ± 0.9(5)	9.6
A2	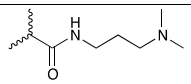	29.1 ± 0.2(5)	-
AO2	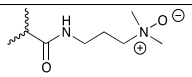	26.4 ± 1.6	2.7
A3	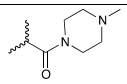	35.3 ± 1.0	-
AO3	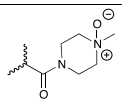	28.3 ± 1.9	7
A4	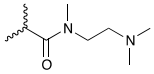	34.4 ± 0.3	-
AO4	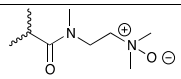	31.7 ± 0.8	2.7
A5	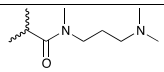	37.3 ± 1.1	-
AO5	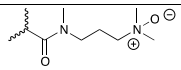	36 ± 0.3(5)	1.3

Table 2 Average contact angle, ± standard deviation (SD) and the difference (Δ) for tertiary amines and corresponding amine oxides representing change in hydrophilicity measured for functionalized silicon wafers.

3.5 Properties of the surfaces assessed by Atomic Force Microscopy

AFM imaging of the HF-etched silicon surfaces reveals a significantly smoother surface with some local areas of much greater height which we ascribe to small regions of remaining silicon oxide (**Figure 5**). After immobilization of the tertiary amines and amine *N*-oxides the surfaces appear more highly textured (**Figure 6**) than the freshly etched silicon, reminiscent of the native silicon seen in **Figure 5(a)**.

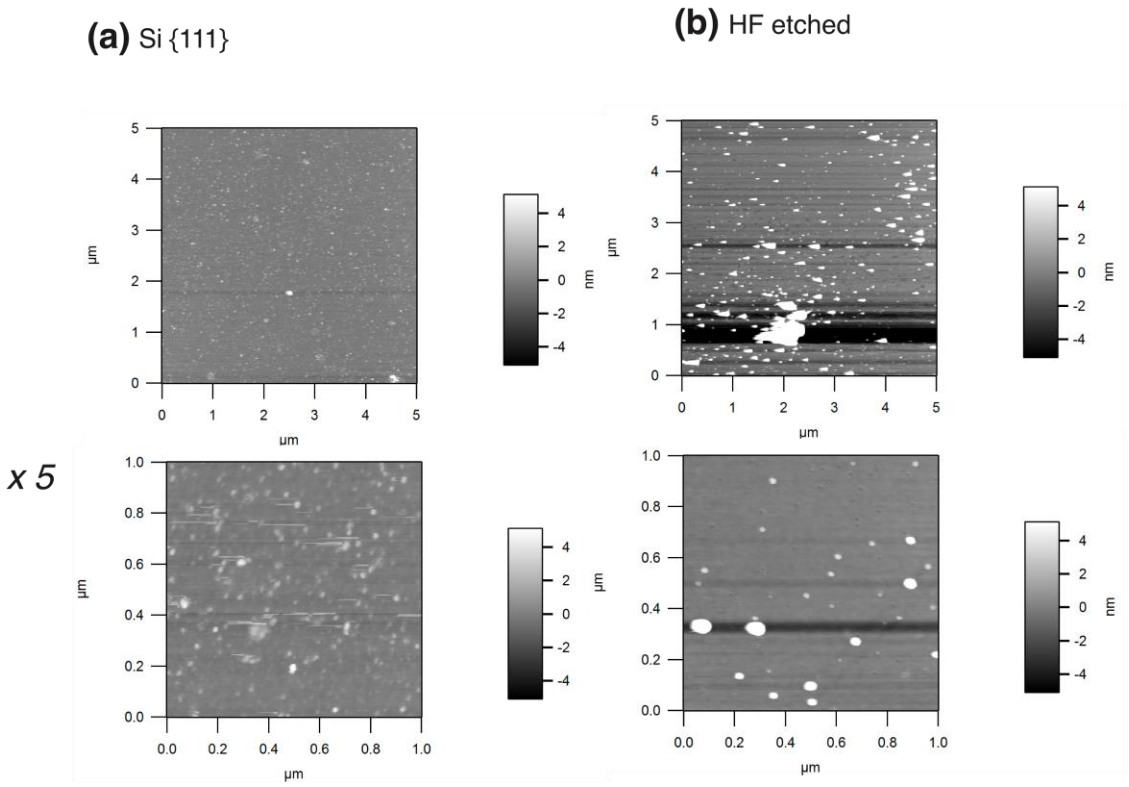

Figure 5 AFM images for (a) native silicon {111}, (b) etched silicon. The upper images are 5 x 5 μm and the lower magnifications 1 x 1 μm, with a height scale of ±5 nm in both cases.

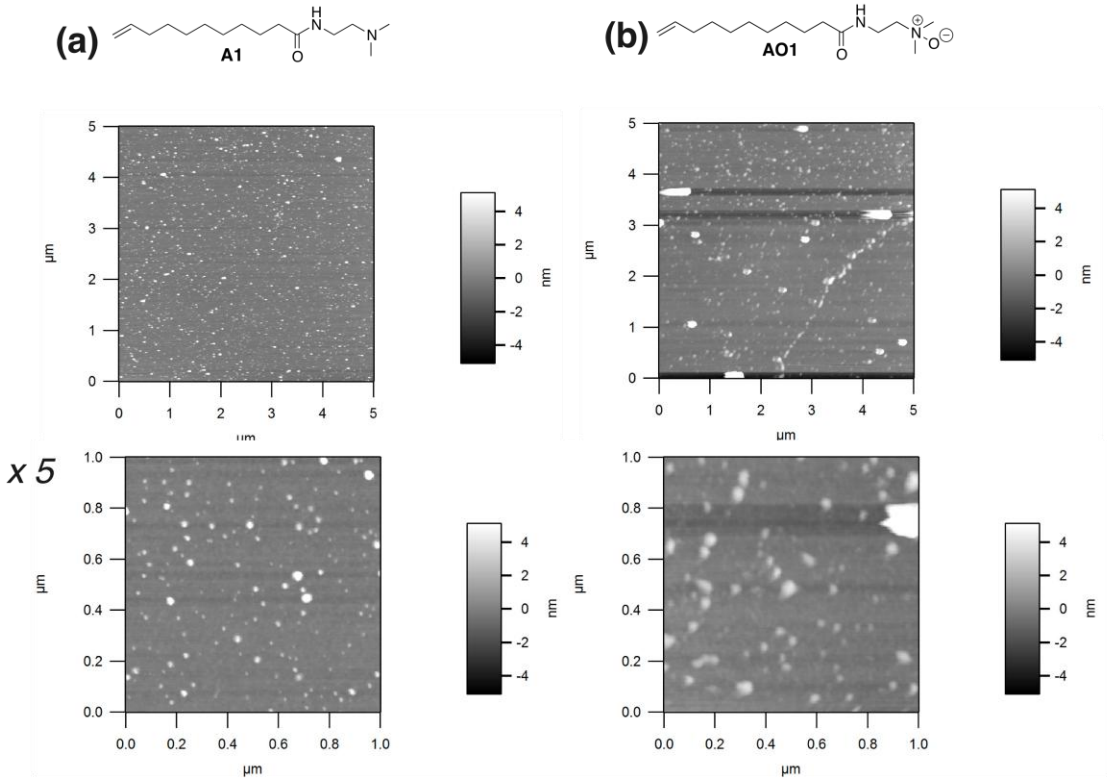

Figure 6 AFM images for (a) surface functionalized with amine **A1**, (b) surface functionalized with amine *N*-oxide **AO1**. The upper images are 5 x 5 μm and the lower magnifications 1 x 1 μm, with a height scale of ±5 nm in both cases.

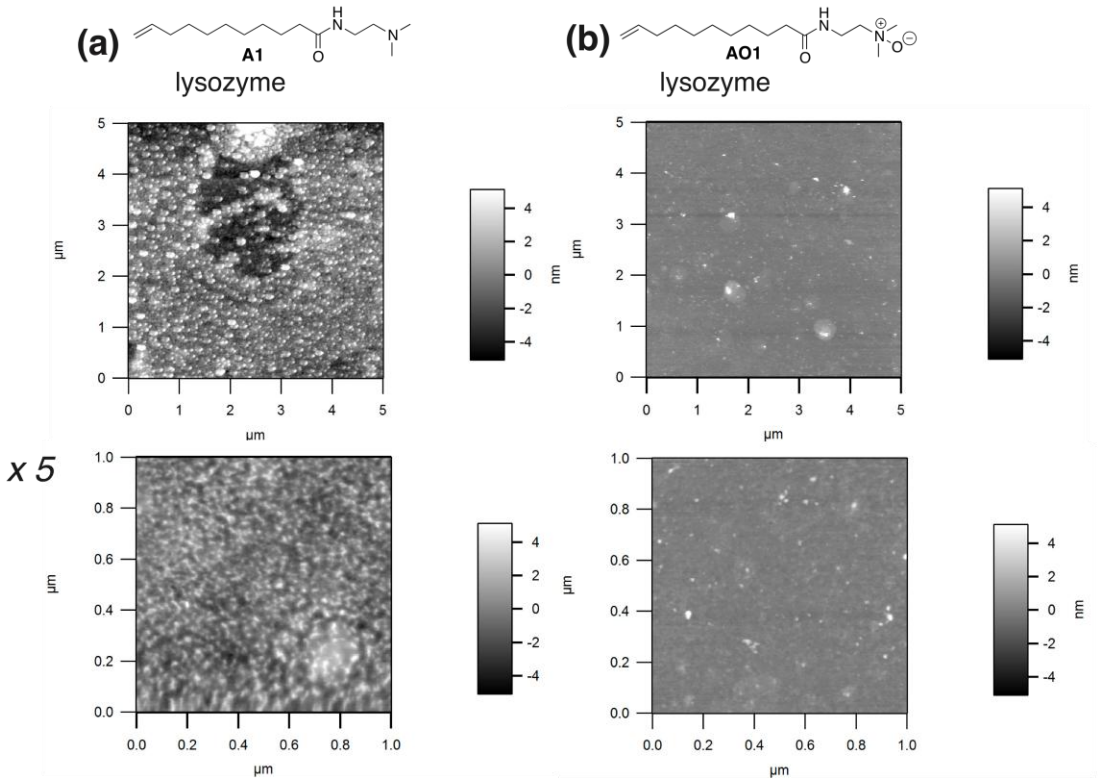

Figure 7 AFM images for (a) deposition of lysozyme on silicon functionalized with amine **A1**, (b) deposition of lysozyme on silicon functionalized with amine *N*-oxide **AO1**. The upper images are 5 x 5 μm and the lower magnifications 1 x 1 μm, with a height scale of ±5 nm in both cases.

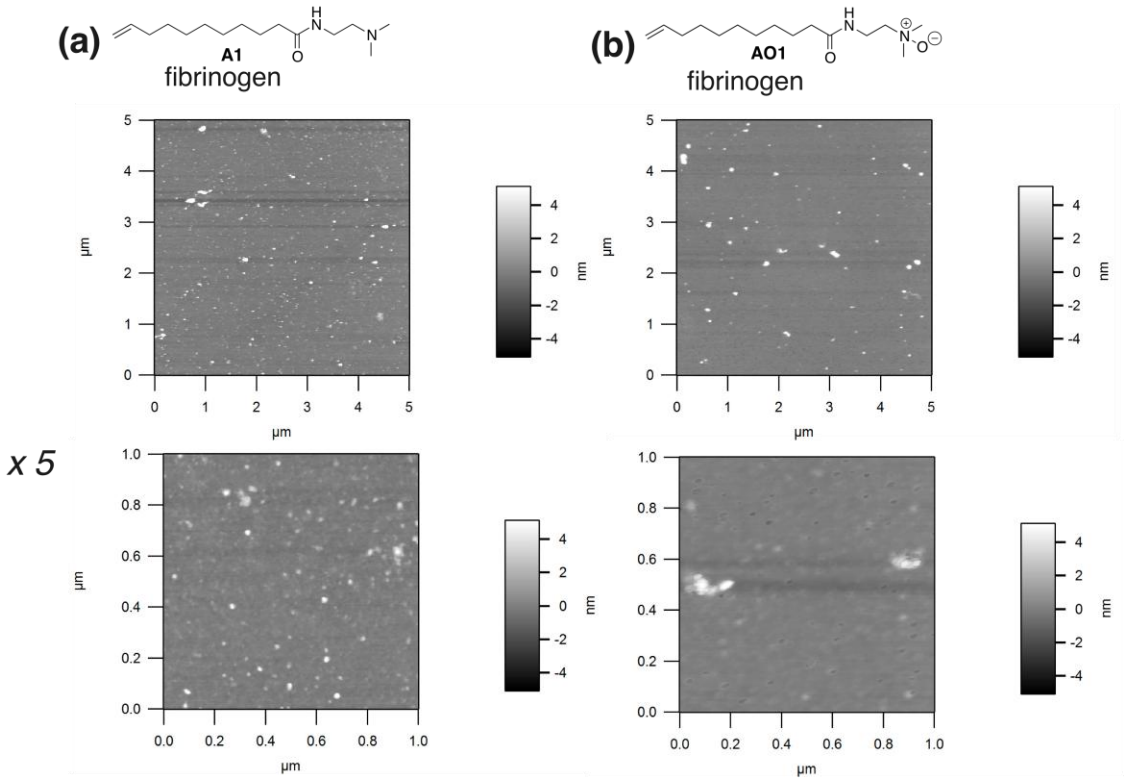

Figure 8 AFM images for (a) deposition of fibrinogen on silicon functionalized with amine **A1**, (b) deposition of fibrinogen on silicon functionalized with amine *N*-oxide **AO1**. The upper images are 5 x 5 μm and the lower magnifications 1 x 1 μm, with a height scale of ±5 nm in both cases.

The *N*,*N*-dimethylamine *N*-oxide that has previously been observed to be most resistant to non-specific adhesion[13] was imaged before and after exposure to protein and rinsing. Tertiary amine **A1** is seen to adsorb significantly more lysozyme (**Figure 7**) compared to its corresponding tertiary amine *N*-oxide **AO1**, with densely populated spherical objects of approximately 100 nm diameter deposited from 1 mM lysozyme solution onto the amine-functionalized surface (**Figure 7(a)**). In agreement with our previous imaging work on tertiary amine self-assembled

monolayers on gold surfaces,[13] we believe these to be too large to represent individual lysozyme molecules which are known to have dimensions in solution of 2.5 x 2.5 x 6 nm,[37] but may be aggregates of lysozyme minimizing their exposed surface area at the interface. **Figure 8 (b)** appears to show a lower density of fibrinogen molecules adsorbed from the less concentrated 1 μM solution with a relatively smooth surface evident (**Figure 9**). The root mean square roughness of the amine surface **A1** coated with lysozyme is 4 nm, whereas the same protein deposited on a surface decorated with amine *N*-oxide **AO1 Figure 6 (b)** has a surface roughness of <1 nm (**Figure 9)**.

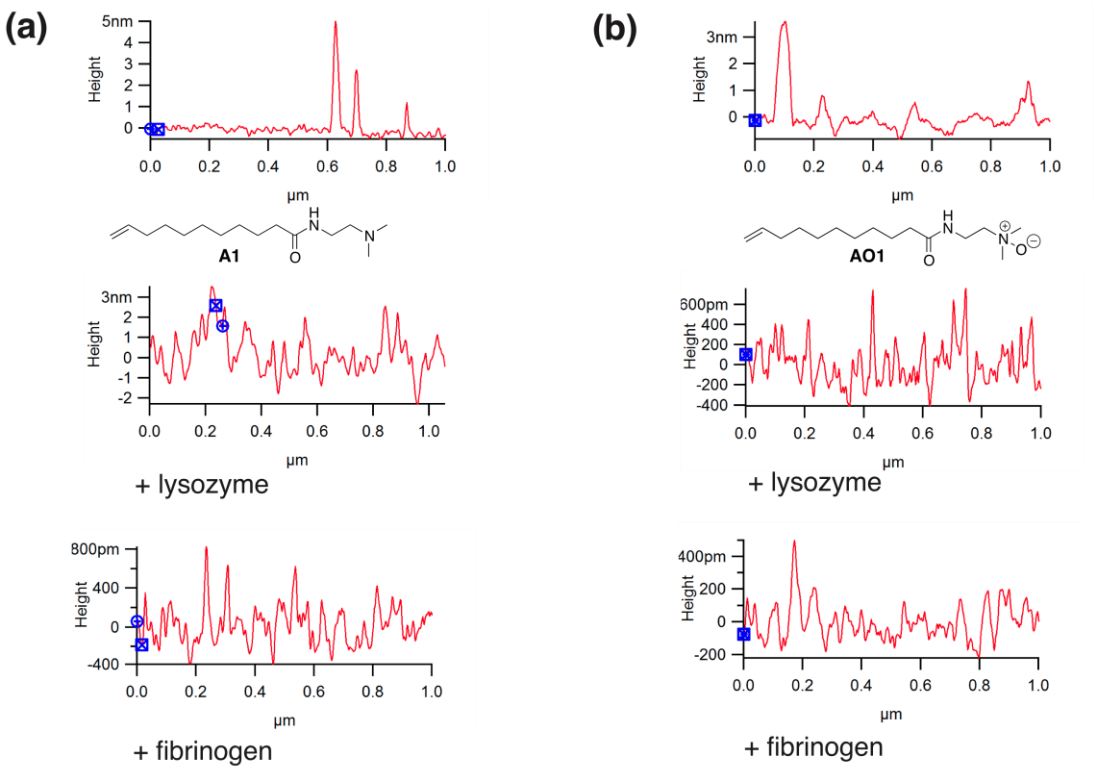

Figure 9 AFM cross-section profiles for (a) silicon functionalized with amine **A1**, (b) deposition silicon functionalized with amine *N*-oxide **AO1**, and subsequent deposition of either lysozyme or fibrinogen on each surface.

Taken together with our previous results, wherein we used the more challenging *in situ* chemical oxidation of the amine to prepare the tertiary *N*-oxides, these data indicate that any possible oxidation of the underlying substrate during that process is not responsible for the difference in protein adhesion observed. In addition, the monolayer on the underlying silicon substrate appears by AFM to give a dramatic reduction in non-specific protein binding.

4. SUMMARY AND CONCLUSIONS

The preparation of ω-alkenyl tertiary amine *N*-oxides in solution is shown herein to be a straightforward process that allows access to high quality monolayers on silicon {111} surfaces. Whilst corresponding tertiary amine *N*-oxides on gold – thiol self-assembled monolayers allow the study of kinetic processes (for example by quartz crystal microbalance or similar methods),[13] the ease of preparation and quality of the silicon surfaces and associated monolayers in this new work offer significant practical advantage, as well as reduction in non-specifically adsorbed protein. Consistent with our previous work on gold – thiol self-assembled monolayers, the new tertiary amine *N*-oxides adsorb far less lysozyme or fibrinogen than corresponding tertiary amines under the same conditions of pH and temperature. The ability to prepare silicon surfaces with very different protein, and potentially cell-adhesion properties, will find application in sensors and for cell-growth applications. We are especially interested in using high throughput screens[38] to uncover new materials compatible with *Archeae* biofilm formation. Tertiary amine functionality forms a key component of several commercial resin beads and other polymers, including poly-dimethylaminomethacrylate that are used in biotechnology and these results reinforce the potential of a straightforward oxidative step in finding new applications for these

materials. In summary, we prepare a set of new ω-tertiary amine *N*-oxides and show how their immobilization on hydrofluoric acid-etched silicon leads to a significant reduction in non-specific adsorption of the model proteins lysozyme and fibrinogen at the interface.

ASSOCIATED CONTENT

Supporting Information.

Low-resolution XPS spectra for native and etched silicon surfaces, tensiometry data for compounds **A1**-**A5**, ^{1}H and ^{13}C NMR spectra for compounds **A1**-**A5** and **AO1**-**AO5**.

AUTHOR INFORMATION

Corresponding Author

*E-mail: a.marsh@warwick.ac.uk.

‡ Undergraduate Research Project Student (ALC 2009-10, TH 2012 ERASMUS Exchange from Université Catholique de Louvain).

The authors declare no competing financial interest.

ACKNOWLEDGEMENTS

We thank the Warwick BBSRC DTC and the Perry Foundation for a studentship and funding to D.A.D. H.S. thanks EPSRC for a studentship. The drop shape analyzer used in this research were obtained through Birmingham Science City: Innovative Uses for Advanced Materials in the Modern World with support from Advantage West Midlands (AWM) and part funded by the European Regional Development Fund (ERDF). We thank Professor Tim S. Jones for access to the Atomic Force Microscope and EPSRC for funding this instrument.

REFERENCES

1. Halik, M.; Hirsch, A., The Potential of Molecular Self-Assembled Monolayers in Organic Electronic Devices. *Adv. Mater.* **2011,** 23, (22-23), 2689-2695.
2. Lin, V. S.-Y.; Motesharei, K.; Dancil, K.-P. S.; Sailor, M. J.; Ghadiri, M. R., A Porous Silicon-Based Optical Interferometric Biosensor. *Science* **1997,** 278, (5339), 840-843.
3. Jane, A.; Dronov, R.; Hodges, A.; Voelcker, N. H., Porous silicon biosensors on the advance. *Trends Biotechnol.* **2009,** 27, (4), 230-239.
4. Jonkheijm, P.; Weinrich, D.; Schroder, H.; Niemeyer, C. M.; Waldmann, H., Chemical Strategies for Generating Protein Biochips. *Angew. Chem. Int. Ed. Engl.* **2008,** 47, (50), 9618-9647.
5. Nguyen, A. T.; Baggerman, J.; Paulusse, J. M. J.; van Rijn, C. J. M.; Zuilhof, H., Stable Protein-Repellent Zwitterionic Polymer Brushes Grafted from Silicon Nitride. *Langmuir* **2011,** 27, (6), 2587-2594.
6. Rothemund, P. W. K., Folding DNA to create nanoscale shapes and patterns. *Nature* **2006,** 440, (7082), 297-302.
7. Maruccio, G.; Visconti, P.; Arima, V.; D'Amico, S.; Biasco, A.; D'Amone, E.; Cingolani, R.; Rinaldi, R.; Masiero, S.; Giorgi, T.; Gottarelli, G., Field Effect Transistor Based on a Modified DNA Base. *Nano Letters* **2003,** 3, (4), 479-483.
8. Olivier, A.; Meyer, F.; Desbief, S.; Verge, P.; Raquez, J.-M.; Lazzaroni, R.; Damman, P.; Dubois, P., Reversible positioning at submicrometre scale of carbon nanotubes mediated by pH-sensitive poly(amino-methacrylate) patterns. *Chem. Commun.* **2011,** 47, (4), 1163-1165.
9. Kuo, C.-H.; Liu, C.-P.; Lee, S.-H.; Chang, H.-Y.; Lin, W.-C.; You, Y.-W.; Liao, H.-Y.; Shyue, J.-J., Effect of surface chemical composition on the work function of silicon substrates modified by binary self-assembled monolayers. *Phys. Chem. Chem. Phys.* **2011,** 13, (33), 15122-15126.
10. Su, W.; Bonnard, V.; Burley, G. A., DNA-Templated Photonic Arrays and Assemblies: Design Principles and Future Opportunities. *Chem.-Eur. J.* **2011,** 17, (29), 7982-7991.
11. Banerjee, I.; Pangule, R. C.; Kane, R. S., Antifouling Coatings: Recent Developments in the Design of Surfaces That Prevent Fouling by Proteins, Bacteria, and Marine Organisms. *Adv. Mater.* **2011,** 23, (6), 690-718.
12. Dilly, S. J.; Beecham, M. P.; Brown, S. P.; Griffin, J. M.; Clark, A. J.; Griffin, C. D.; Marshall, J.; Napier, R. M.; Taylor, P. C.; Marsh, A., Novel tertiary amine oxide surfaces that resist nonspecific protein adsorption. *Langmuir* **2006,** 22, (19), 8144-8150.
13. Dobrzanska, D. A.; Cooper, A. L.; Dowson, C. G.; Evans, S. D.; Fox, D. J.; Johnson, B. R.; Moore, C. I.; Randev, R. K.; Stec, H. M.; Taylor, P. C.; Marsh, A., Conversion of protein-adhesive surfaces into protein-resistant tertiary amine N-oxides. *Langmuir* **2012** submitted.
14. Singh, S. K.; Bajpai, M.; Tyagi, V. K., Amine Oxides: A Review. *J. Oleo. Sci.* **2006,** 55, (3), 99-119.
15. Goracci, L.; Germani, R.; Savelli, G.; Bassani, D. M., Hoechst 33258 as a pH-sensitive probe to study the interaction of amine oxide surfactants with DNA. *Chembiochem* **2005,** 6, (1), 197-203.
16. Bordi, F.; Cerichelli, G.; de Berardinis, N.; Diociaiuti, M.; Giansanti, L.; Mancini, G.; Sennato, S., Synthesis and Physicochemical Characterization of New Twin-Tailed N-Oxide Based Gemini Surfactants. *Langmuir* **2010,** 26, (9), 6177-6183.
17. Chae, P. S.; Laible, P. D.; Gellman, S. H., Tripod amphiphiles for membrane protein manipulation. *Mol. Biosyst.* **2010,** 6, (1), 89-94.

18. Bernier, D.; Wefelscheid, U. K.; Woodward, S., Properties, Preparation and Synthetic Uses of Amine N-Oxides. An Update. *Org. Prep. Proced. Int.* **2009,** 41, (3), 173-210.
19. Beecham, M. P. Supramolecular Chaperones to Assist Protein Folding. University of Warwick, Coventry, 2005.
20. Buriak, J. M., Organometallic chemistry on silicon surfaces: formation of functional monolayers bound through Si-C bonds. *Chem. Commun.* **1999**, (12), 1051-1060.
21. Buriak, J. M., Organometallic Chemistry on Silicon and Germanium Surfaces. *Chem. Rev.* **2002,** 102, (5), 1271-1308.
22. Lasseter, T. L.; Clare, B. H.; Abbott, N. L.; Hamers, R. J., Covalently Modified Silicon and Diamond Surfaces: Resistance to Nonspecific Protein Adsorption and Optimization for Biosensing. *J. Am. Chem. Soc.* **2004,** 126, (33), 10220-10221.
23. Li, Y.; Calder, S.; Yaffe, O.; Cahen, D.; Haick, H.; Kronik, L.; Zuilhof, H., Hybrids of Organic Molecules and Flat, Oxide-Free Silicon: High-Density Monolayers, Electronic Properties, and Functionalization. *Langmuir* **2012,** 28, (26), 9920-9929.
24. El-Faham, A.; Albericio, F., Peptide Coupling Reagents, More than a Letter Soup. *Chem. Rev.* **2011,** 111, (11), 6557-6602.
25. Montalbetti, C. A. G. N.; Falque, V., Amide bond formation and peptide coupling. *Tetrahedron* **2005,** 61, (46), 10827-10852.
26. Balamurugan, S.; Kannan, P., Synthesis and characterization of symmetrical banana shaped liquid crystalline polyethers. *J. Mol. Struct.* **2009,** 934, (1,Äì3), 44-52.
27. Cane, D. E.; Yang, G.; Coates, R. M.; Pyun, H. J.; Hohn, T. M., Trichodiene synthase. Synergistic inhibition by inorganic pyrophosphate and aza analogs of the bisabolyl cation. *J. Org. Chem.* **1992,** 57, (12), 3454-3462.
28. Grigoropoulou, G.; Clark, J. H., A catalytic, environmentally benign method for the epoxidation of unsaturated terpenes with hydrogen peroxide. *Tetrahedron Lett.* **2006,** 47, (26), 4461-4463.
29. Puniredd, S. R.; Assad, O.; Haick, H., Highly stable organic monolayers for reacting silicon with further functionalities: The effect of the C-C bond nearest the silicon surface. *J. Am. Chem. Soc.* **2008,** 130, (41), 13727-13734.
30. Lehner, A.; Steinhoff, G.; Brandt, M. S.; Eickhoff, M.; Stutzmann, M., Hydrosilylation of crystalline silicon (111) and hydrogenated amorphous silicon surfaces: A comparative x-ray photoelectron spectroscopy study. *J. Appl. Phys.* **2003,** 94, (4), 2289-2294.
31. Baio, J. E.; Weidner, T.; Brison, J.; Graham, D. J.; Gamble, L. J.; Castner, D. G., Amine terminated SAMs: Investigating why oxygen is present in these films. *J. Electron Spectrosc. Relat. Phenom.* **2009,** 172, (1), 2-8.
32. Wagner, C. D., *Handbook of X-Ray Photoelectron Spectroscopy*. Perkin-Elmer Corporation: 1979.
33. Yaffe, O.; Scheres, L.; Segev, L.; Biller, A.; Ron, I.; Salomon, E.; Giesbers, M.; Kahn, A.; Kronik, L.; Zuilhof, H.; Vilan, A.; Cahen, D., Hg/Molecular Monolayer,àíSi Junctions: Electrical Interplay between Monolayer Properties and Semiconductor Doping Density. *J. Phys. Chem. C* **2010,** 114, (22), 10270-10279.
34. Jansen, R. J. J.; van Bekkum, H., XPS of nitrogen-containing functional groups on activated carbon. *Carbon* **1995,** 33, (8), 1021-1027.
35. Barazzouk, S. Ø.; Daneault, C., Amino Acid and Peptide Immobilization on Oxidized Nanocellulose: Spectroscopic Characterization. *Nanomaterials* **2012,** 2, (2), 187-205.

36. Metwalli, E.; Haines, D.; Becker, O.; Conzone, S.; Pantano, C. G., Surface characterizations of mono-, di-, and tri-aminosilane treated glass substrates. *J. Colloid Interf. Sci.* **2006,** 298, (2), 825-831.
37. Krigbaum, W. R.; Kuegler, F. R., Molecular conformation of egg-white lysozyme and bovine alpha-lactalbumin in solution. *Biochemistry* **1970,** 9, (5), 1216-1223.
38. Pernagallo, S.; Wu, M.; Gallagher, M. P.; Bradley, M., Colonising new frontiers-microarrays reveal biofilm modulating polymers. *J. Mater. Chem.* **2011,** 21, (1), 96-101.

Graphical abstract.